Available online at www.sciencedirect.com
ScienceDirect
Ceramics International 38 (2012) 973–979
CERAMICS INTERNATIONAL
www.elsevier.com/locate/ceramint

Synthesis and characterization of nano-crystalline strontium hexaferrite using the co-precipitation and microemulsion methods with nitrate precursors

A. Drmota [a,*], M. Drofenik [b,c], A. Žnidaršič [a,c]

[a] Nanotesla Institute Ljubljana, Stegne 29, SI-1521 Ljubljana, Slovenia
[b] Faculty of Chemistry and Chemical Engineering, Smetanova ulica 17, 2000 Maribor, Slovenia
[c] CO NAMASTE, Jamova cesta 39, 1000 Ljubljana, Slovenia

Received 13 April 2011; accepted 1 August 2011
Available online 17 August 2011

Abstract

Nano-crystalline strontium hexaferrite ($SrFe_{12}O_{19}$) powder was synthesized using the classical co-precipitation and microemulsion methods. The precursors were obtained by precipitating Sr^{2+} and Fe^{2+} ions using tetramethylammonium hydroxide and calcinating at different temperatures ranging from 400 °C to 1000 °C in air. The influence of the Sr^{2+}/Fe^{3+} mol ratio and the calcination temperature on the product formation and magnetic properties were studied. The formation of nanosized particles of $SrFe_{12}O_{19}$ with a relatively high saturation magnetization M_s = 64 Am^2/kg, remanent magnetization of M_r = 39 Am^2/kg and a coercitivity of H_c = 5.5 kOe was achieved at a Sr^{2+}/Fe^{3+} mol ratio of 1:8 calcined at 900 °C. The formation of the $SrFe_{12}O_{19}$ was inspected using XRD analysis, thermogravimetric analysis (TGA), differential thermal analysis (DTA), TEM, and magnetic measurements.

Keywords: C. Magnetic properties; Nano-crystalline strontium hexaferrite; Chemical preparation

1. Introduction

Nano-crystalline strontium hexaferrite ($SrFe_{12}O_{19}$) powder is a promising material for use as microwave absorbers in the gigahertz (GHz) range due to its high saturation magnetization, high coercitivity (which mainly originates from its high magnetocrystalline anisotropy), high electrical resistivity and because of its low dielectric and magnetic losses in the microwave frequency band [1–4].

The classical technique to synthesize $SrFe_{12}O_{19}$ using a solid-state reaction by mixing the oxide/carbonate and then calcining at temperatures higher than 1200 °C has some disadvantages, such as chemical inhomogeneity, a coarser particle size and impurities due to subsequent ball milling. For this reason, it is important to develop techniques by which the size, shape and chemical homogeneity of the particles can be well controlled [5]. Numerous nonconventional techniques, such as the co-precipitation method [6], the microemulsion method [4], the glass crystallization method [7], the self-propagating high-temperature synthesis method [8], the hydrothermal method [9], mechanical alloying [10] and the sol–gel method [11], were used to prepare ultrafine and monodispersed $SrFe_{12}O_{19}$ particles with high crystallinity.

The objective of the present work was to study the influence of the Sr^{2+}/Fe^{3+} mol ratio and the calcination temperature on the chemistry of the phase formation and the magnetic properties of Sr-hexaferrite particles obtained via the chemical co-precipitation and microemulsion methods using nitrate precursors.

2. Experimental

2.1. Chemicals

The chemicals used for the syntheses of the different samples were strontium nitrate anhydrous ($Sr(NO_3)_2$), 98%, Alfa Aesar, iron (III) nitrate nonahydrate ($Fe(NO_3)_3{\cdot}9H_2O$), ACS, 98.0–101.0%, Alfa Aesar; tetramethylammonium

* Corresponding author. Tel.: +386 1 58 33 134; fax: +386 1 58 33 232.
E-mail address: ana.drmota@kolektor.com (A. Drmota).

0272-8842/$36.00
doi:10.1016/j.ceramint.2011.08.018

hydroxid solution 25% (TMAH) ($C_4H_{13}NO$), Applichem; cyclohexane (C_6H_{12}), ACS, 99+%, Alfa Aesar; sodium n-dodecyl sulfate (SDS) ($CH_3(CH_2)_{11}OSO_3Na$), 99%, Sigma Aldrich; 1-butanol ($CH_3(CH_2)_3OH$), 99%, Alfa Aesar and ethanol (CH_3CH_2OH), 96%, Riedel-de Haën.

2.2. Synthesis procedure

The co-precipitation method and the microemulsion method were applied for the preparation of the $SrFe_{12}O_{19}$ precursors. Prior to the synthesis, aqueous solutions of strontium and iron nitrate with various Sr^{2+}/Fe^{3+} mol ratios (1:6.4, 1:8, 1:10 and 1:12) were prepared. Although a mol ratio of 1:12 should be sufficient, according to the stoichiometry, an excess of strontium nitrate was necessary because the strontium hydroxide is partially soluble in water [9].

In the co-precipitation method the Sr(II) and Fe(III) hydroxide precursors were precipitated during the reaction between the aqueous solution of metal nitrates and the 0.5-M aqueous solution of tetramethylammonium hydroxide (TMAH), which served as a precipitating agent (Table 1). The precipitation was performed at room temperature and a pH value of 12.7. The brownish precipitates were washed several times with a mixture of distilled water and ethanol (volume ratio 1:1) and dried at 100 °C.

The microemulsion system used in this study consisted of sodium n-dodecyl sulfate (SDS) as the surfactant, 1-butanol as the cosurfactant, cyclohexane as the continuous oil phase and an aqueous solution of reactants as the dispersed phase. Two microemulsions (I and II) with identical compositions and different reagents in the aqueous phase were prepared (Table 2). The aqueous phase in microemulsion I comprised a mixture of strontium and iron nitrate aqueous solutions. The aqueous phase in microemulsion II comprised a 0.5-M solution of tetramethylammonium hydroxide (TMAH), which served as a precipitation agent. The brownish precipitates of metal hydroxides appeared within the nanosized aqueous droplets after the two microemulsions were mixed at room temperature and pH 13.5. The precipitates were washed several times with a mixture of distilled water and ethanol (volume ratio 1:1) and dried at 100 °C.

Finally, these dried precursor powders prepared with different Sr^{2+}/Fe^{3+} mol ratios were calcined at different temperatures (400–1000 °C) for 1 h with a heating/cooling rate of 5 °C/min. The calcinations were performed in a sample holder in the TG apparatus in a static atmosphere with a precise control of the weight change and the calcination temperature.

Table 1
The composition of a typical co-precipitation system used for the synthesis of the precursor with a Sr^{2+}/Fe^{3+} mol ratio of 1/8.

	Aqueous solution	Wt.%
Metal nitrates	0.01 M $Sr(NO_3)_2$ + 0.08 M $Fe(NO_3)_3$	50
Precipitation agent	0.5 M TMAH	50

Table 2
The composition of the microemulsion system used for the synthesis of the precursor with a Sr^{2+}/Fe^{3+} mol ratio of 1/8.

	Microemulsion I	Microemulsion II	Wt.%
Aqueous phase	0.01 M $Sr(NO_3)_2$ + 0.08 M $Fe(NO_3)_3$	0.5 M TMAH	30
Surfactant	SDS	SDS	13
Cosurfactant	1-Butanol	1-Butanol	17
Oil phase	Cyclohexane	Cyclohexane	35

2.3. Characterization

The dried precursors were characterized using thermogravimetric analyses (TGA) and differential thermal analyses (DTA) in air with a heating/cooling rate of 5 °C/min. The morphology of the powders after the calcination was investigated with transmission electron microscopy (TEM). The size of the nanoparticles was measured with dynamic light-scattering particle size analyses (DLS) and from the powders' specific surface A_s using the BET method and estimated using the relation $D_{BET} = 6\rho/A_s$, where $\rho = 5.1$ g/cm^3 for spherical particles. The magnetic measurements of the calcined samples were carried out using a magneto-susceptometer (DSM-10).

3. Results and discussion

3.1. Thermal analysis

Typical TGA and DTA curves of the dried precursors prepared with the co-precipitation method and the microemulsion method at a Sr^{2+}/Fe^{3+} mol ratio of 1:8 are shown in Fig. 1.

The DTA curves of the samples prepared by the co-precipitation method show an endothermic peak at 116 °C and two exothermic peaks at 262 °C and 719 °C. The endothermic peak was attributed to the vaporization of the water from the precursor. On the other hand, the first exothermic peak was ascribed to the disintegration-oxidation of the residual organic precipitation agent in air at elevated temperatures. The second exothermic pick was attributed to the formation enthalpy and/or subsequent crystallization of the hexaferrite ($SrFe_{12}O_{19}$).

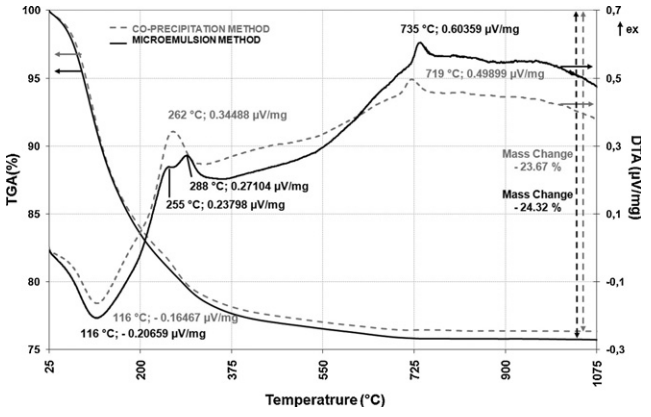

Fig. 1. DTA and TGA of precursor with the Sr^{2+}/Fe^{3+} mol ratio 1:8 prepared by the co-precipitation and microemulsion methods.

In the case that the precursor was prepared by co-precipitation in a microemulsion, the DTA curve indicated an endothermic peak at 116 °C and three exothermic peaks at 255 °C, 288 °C and 735 °C. Here, the endothermic peak is a consequence of the vaporization of the residual solvent and the water from the precursor. While the appearance of two close but separate exothermic peaks between 255 °C and 288 °C is consistent with the chosen method of synthesis, where we used two different organic agents, i.e., in addition to an organic precipitation agent (TMAH), an organic surfactant (SDS) was also applied. However, both of them exhibited different disintegration temperatures. The third exothermic peak at around 735 °C could, like in the former case, be attributed to the formation of crystalline $SrFe_{12}O_{19}$.

The TGA showed a continuous weight loss from room temperature to about 730 °C. Theoretically, the transformation of the dried precursor hydroxides $Sr(OH)_2$ and $Fe(OH)_3$ into their oxides SrO and Fe_2O_3 and further into the hexagonal ferrite structure, at a Sr^{2+}/Fe^{3+} mol ratio of 1:8, during the calcination in air led to a weight loss of around 24%, which is in good agreement with the experimental results (Fig. 1).

3.2. Phase analysis and crystalline structure

In order to investigate the effect of the calcination temperature on the formation of $SrFe_{12}O_{19}$ powders, a series of experiments was carried out on co-precipitated samples and those prepared in microemulsions at various calcination temperatures, ranging from 600 to 1000 °C, for a precursor Sr^{2+}/Fe^{3+} mol ratio of 1:6.4. Figs. 2 and 3 show the XRD patterns of these samples.

The XRD patterns of the produced powders showed the presence of Sr-hexaferrite $SrFe_{12}O_{19}$, strontium peroxide SrO_2, hematite Fe_2O_3, and magnetite Fe_3O_4 phases depending on the calcination temperature and the method of synthesis.

At a low temperature of 600 °C, powder prepared by co-precipitation contained a nonmagnetic phase hematite Fe_2O_3, while the powder prepared with the microemulsion method

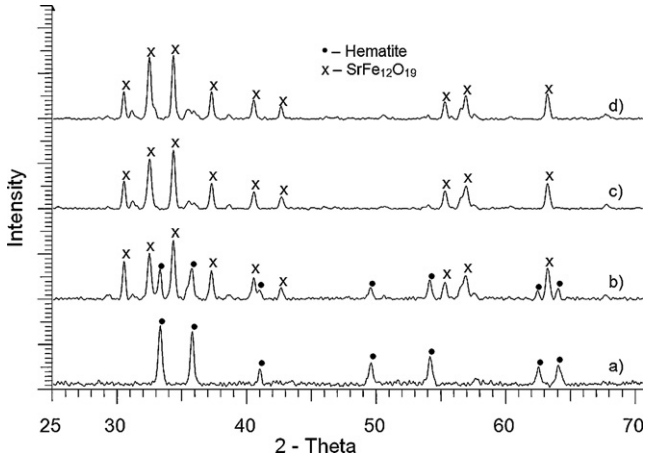

Fig. 2. XRD spectra of co-precipitated samples with a Sr^{2+}/Fe^{3+} mol ratio of 1:6.4 calcined at temperatures: (a) 600 °C, (b) 800 °C, (c) 900 °C and (d) 1000 °C for 1 h.

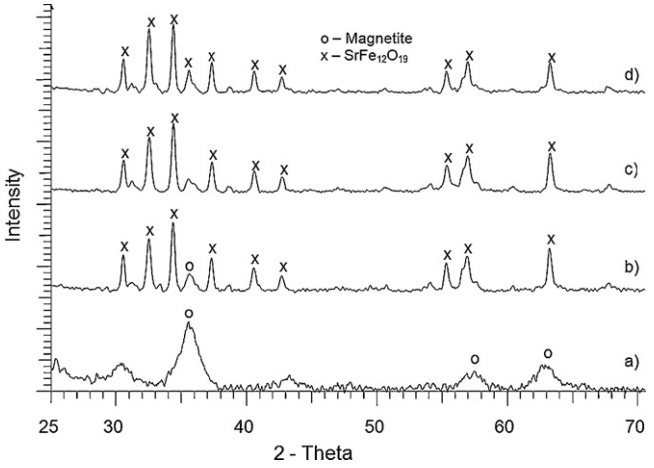

Fig. 3. XRD spectra of samples prepared by the microemulsion method with a Sr^{2+}/Fe^{3+} mol ratio of 1:6.4 calcined at temperatures: (a) 600 °C, (b) 800 °C, (c) 900 °C and (d) 1000 °C for 1 h.

contained the magnetic phase magnetite. Here, the temperature to form the Sr-hexaferrite is too low, while on the other hand the second constitutive phase SrO is, in spite of its large excess at low calcinations temperatures, not observed due to its low crystallinity.

The formation of two different forms of iron oxides during the calcinations at 600 °C, i.e., hematite after the co-precipitation was used and magnetite when the microemulsion method was applied, can be explained by the difference in the preparation method. The precipitation reaction should be slower in a reverse micelle medium, when considering the necessary coupling of the rate constant of the chemical reaction and the rate constant of the fusion of the reverse micelles, which must happen prior to the particular reaction [12].

The slower rate of the precipitation when the synthesis is performed within the reverse micelles, which leads to a compartmentalization of the bulk compared to that in the bulk conditions, could lead to the formation of $Fe_2O_3 \cdot H_2O$, which on further heating might yield a magnetic phase maghemite/magnetite. However, the main condition that is crucial for the formation of magnetite is the presence of organic aids, which during heating at elevated temperatures prior to the complete oxidation and the formation of carbon oxide, ensures the reduction conditions that yield the magnetite phase instead of the hematite. Furthermore, the reaction occurs in a closed system of the TG apparatus, where any draught of air was excluded. On the other hand, in co-precipitated and calcined samples the $Fe(OH)_3$ yields hematite.

At a temperature of 800 °C it is mainly the formation of $SrFe_{12}O_{19}$ that can be observed for both types of samples, prepared by co-precipitation and/or by microemulsion-assisted synthesis. This is consistent with the DTA, where the maximum assigned to ferrite formation is observed at 735 °C. Besides, some XRD peaks of hematite Fe_2O_3 in the samples prepared via microemulsion the hematite phase can be detected.

The XRD analysis of the samples calcinated at 900 °C showed the formation of the $SrFe_{12}O_{19}$ phase, with no other phase being detected, Figs. 3 and 4. This sample still has a large

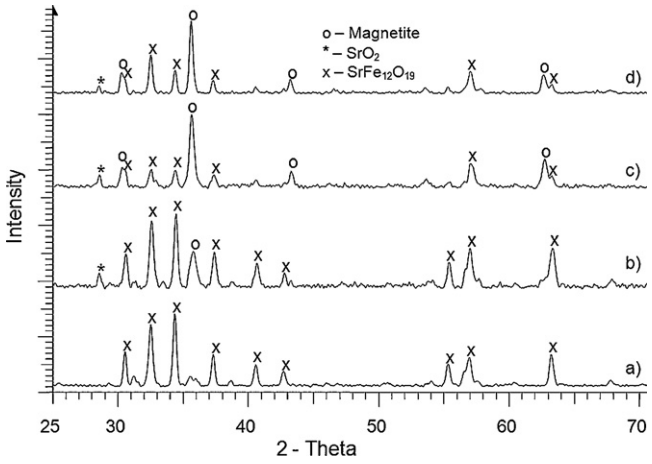

Fig. 4. XRD patterns for samples with various Sr^{2+}/Fe^{3+} mol ratios: (a) 1:6.4, (b) 1:8, (c) 1:10 and (d) 1:12 prepared with the co-precipitation method calcined at 900 °C.

excess of SrO and the temperature is sufficiently high that all of the hematite and/or magnetite in the precursor reacts to form the hexaferrite phase, with the exception of the strontium oxide, which was designed to be in excess due to the partial solubility of the strontium hydroxide in the water/alcohol during the processing of the precursor. The SrO, which is otherwise prone to react with atmospheric moisture and carbon dioxide, forming hydocarbonates with a low crystallinity, can be easily extracted with dilute hydrochloric acid and chemically analyzed, while the Sr-ferrite is poorly soluble in acids. From these results one can conclude that the Sr^{2+}/Fe^{3+} mol ratio of 1:6.4 is a little bit too high, since the excess of free SrO and/or SrO_2 can be chemically analyzed in the calcined samples.

On the other hand, the XRD patterns for the samples calcinated at 1000 °C show identical diffraction patterns to those of the samples calcined at 900 °C. Therefore, one can conclude that the calcination temperature of 900 °C is sufficient for a complete reaction between stoichiometric ratios of the precursor components forming the target phase, i.e., $SrFe_{12}O_{19}$, while the excess of SrO can be easily removed from the product.

In order to complete the range of trial-and-error experiments the samples with Sr:Fe mol ratios of 1:8, 1:10 and 1:12 were calcinated at 900 °C. Here, the influence of a relatively large excess of SrO in the precursor was gradually reduced and the phase formation depending on the calcinations temperature was followed by XRD (Fig. 4) and by measuring the magnetization of the products (Figs. 6 and 7).

Fig. 4 shows the XRD patterns for the samples prepared with the co-precipitation method and Sr^{2+}/Fe^{3+} mol ratios of 1:6.4, 1:8, 1:10 and 1:12. The pure crystalline single-phase $SrFe_{12}O_{19}$ was formed at a Sr:Fe mol ratio of 1:6.4. On the other hand, the XRD patterns of the produced samples at Sr^{2+}/Fe^{3+} mol ratios of 1:8, 1:10 and 1:12 showed, besides strontium peroxide SrO_2, the presence of the magnetite Fe_3O_4 phase.

With a decrease of the relatively large excess of Sr^{2+} the magnetite phase starts to appear, as observed from the XRD spectra and the magnetization measurements, Fig. 6. It is surprising that in spite of an overall large excess of SrO in the precursor the iron oxide phases can be detected in calcined samples with a mol ratio >1:6.4. The magnetite Fe_3O_4 phase in the samples to a great extent determines the magnetic properties, as is clear from the hysteresis curves, Fig. 7. The phase compositions for the samples prepared with the microemulsion method were almost the same. The proposed reason for such a diverse phase formation, depending on the Sr^{2+}/Fe^{3+} mol ratio, is discussed in Section 3.4.

3.3. Particle size and morphology

Fig. 5 shows the TEM images of $SrFe_{12}O_{19}$ particles prepared by the co-precipitation and microemulsion methods, respectively, with a Sr^{2+}/Fe^{3+} mol ratio of 1:8, calcined at 900 °C for 1 h. There were no dramatic differences in both the particle size and morphology when the samples were prepared using different synthesis methods.

The average size of the $SrFe_{12}O_{19}$ particles in the samples with a limited degree of agglomeration is in the range 40–80 nm, from an inspection of the TEM images. However, when we compare this value with that of the average particle size obtained from the BET measurements, i.e., the D_{BET} d_{BET} = 61 nm (19 m^2/g) with the same Sr^{2+}/Fe^{3+} mol ratio, one can conclude that the agglomeration of particles during the processing is not remarkable. Namely, the agglomeration of the particles might strongly decrease the measured total surface

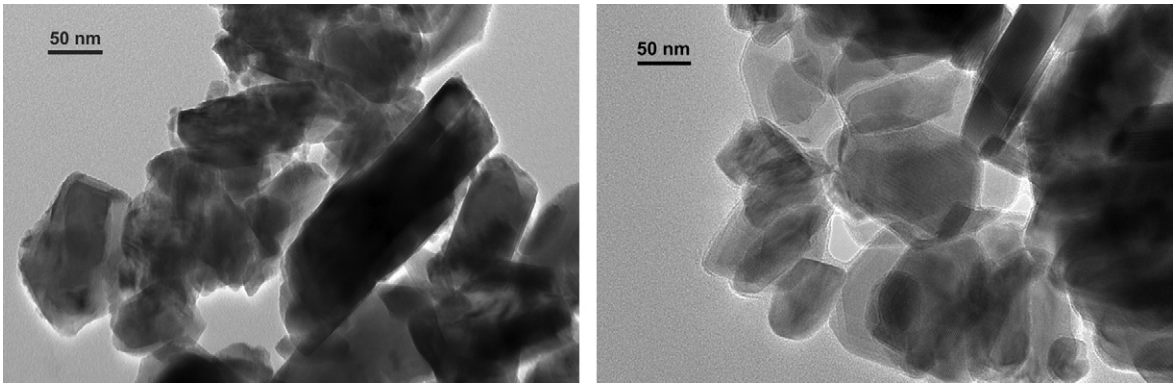

Fig. 5. TEM micrographs of $SrFe_{12}O_{19}$ prepared by the co-precipitation method (left) and the microemulsion method (right).

area and consequently the average particle size estimated from it is consequently apparently larger. The average size of the nanoparticles stabilized in a suspension, i.e., in butylene glycol using a sonificator, was also measured using a dynamic light-scattering particle size analysis (DLS). The results of the DLS analysis showed that the size of the nanoparticles was around 40 nm. Here we must stress that the high energy of the ultrasound radiation breaks the agglomerates and decreases their number. Taking into account the data from the TEM images, the DLS analyses and the BET measurements one can describe the morphology of the synthesized powders as being composed of mostly not agglomerated particles of a size around 40–80 nm.

3.4. Magnetic properties

Here we correlate the results of the magnetization measurements with the phase composition of the studied samples for a constant precursor Sr^{2+}/Fe^{3+} mol ratio heated at temperatures from 600 °C to 1000 °C. The saturation magnetization versus calcination temperature for samples prepared by the co-precipitation and microemulsion methods, with a Sr^{2+}/Fe^{3+} mol ratio of 1:6.4 calcined at different temperatures for 1 h is shown in Fig. 6. Following the magnetization of the product versus the temperature of the calcination we see a gradual increase in the magnetization, which is to be expected, according to the phase composition recorded with XRD spectra, Figs. 2 and 3. At 400 °C the low magnetization mostly reflects the composition of the precursor, where the ferrimagnetic phases were just starting to form but could not be detected in the XRD spectra. They are, however, reflected in a slight magnetization. With an increase of the calcination temperature to about 600 °C the saturation magnetization increased from 4 Am^2/kg at 400 °C to 6 Am^2/kg in the case of the co-precipitation method, and from 10 Am^2/kg to 29 Am^2/kg at 600 °C for the samples prepared from microemulsions. With a further increase in the calcination temperature the magnetization steadily increases to 45 Am^2/kg for the co-precipitated samples and 55 Am^2/kg for the samples from the microemulsion. When the temperature increased to 900 °C and 1000 °C the magnetization of the magnetic particles stays in the range between 50 and 60 Am^2/kg.

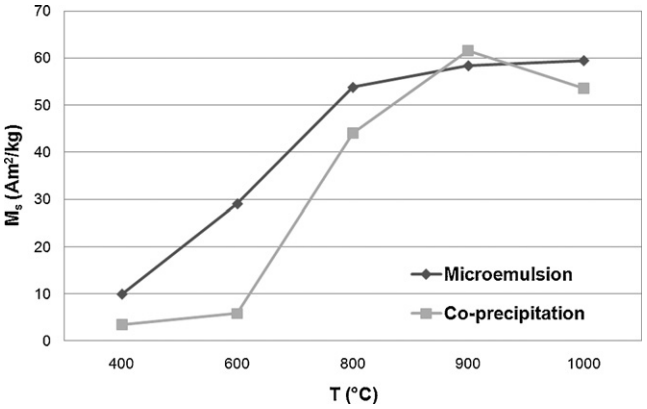

Fig. 6. The saturation magnetization (M_s) of samples prepared by the co-precipitation and microemulsion methods with Sr^{2+}/Fe^{3+} mol ratio 1:6.4 and calcined at different temperatures for 1 h.

The relatively large difference in the saturation magnetization for the co-precipitated and/or the microemulsion synthesized samples calcined at 600 °C are related to the phase composition of the powders examined by XRD analysis. The samples prepared with the co-precipitation method contained hematite, whereas those prepared with the microemulsion method contained the magnetic phase magnetite that increases the magnetization of the otherwise non-magnetic constitutive part (SrO) in the powder calcined at 600 °C. With a further temperature increase the target hexaferrite is being formed Figs. 2 and 3, which increases the magnetization of the calcined products.

Fig. 7 shows the plots of the saturation magnetization (M_s) as a function of the applied field (H_c) for samples prepared by the co-precipitation method and the microemulsion method with different Sr^{2+}/Fe^{3+} mol ratios and calcined at 900 °C for 1 h. Here the shape of the hysteresis loops indicates a drastic change in the phase composition depending on the precursor composition and the temperature.

The samples prepared with Sr^{2+}/Fe^{3+} mol ratios of 1:6.4 and 1:8 exhibited a relatively high saturation magnetization of 64 and 62 Am^2/kg, respectively, and wide hysteresis loops with coercivities of 5.4 and 5.0 kOe and remanent magnetizations of 39 and 36 Am^2/kg, respectively. With decreasing the Sr^{2+}/Fe^{3+}

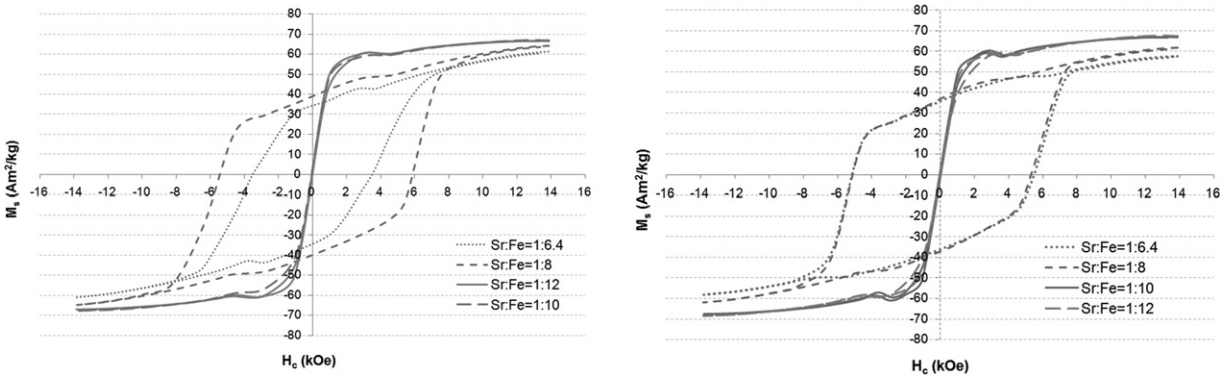

Fig. 7. The hysteresis loops of strontium hexaferrite prepared by the co-precipitation method (left) and the microemulsion method (right) with different Sr^{2+}/Fe^{3+} mol ratios and calcined at 900 °C for 1 h.

mol ratio from 1:8 to 1:10 and/or 1:12 the shape of the hysteresis loop changes drastically, indicating a crucial change in the phase composition, i.e., the magnetic properties of the samples change from high coercivity phases, indicating a hard magnetic character, to a soft magnetic phase. The XRD analysis indicates that the hard magnetic phase is Sr-hexaferrite and the soft magnetic phase is magnetite.

The formation of a submicron-sized strontium hexaferrite, responsible for a nearly square-shaped hysteresis loop in samples with a mol ratio Sr^{2+}/Fe^{3+} of 1:6.4 and 1:8, and a submicron-sized magnetite, exhibiting a hysteresis loop with a very small coercivity, indicating a soft magnetic character in samples with lower Sr^{2+}/Fe^{3+} mol ratios, 1:10 and 1:12, is consistent with the coarsening ability of fine, reactive, iron oxide particles. The essential element of this phenomenon is the fact that the coarsening of the iron particles occurs prior to the onset of the key solid-state reaction, which leads to the target compound. This process is associated with the passivity of the iron oxide particles due to a drastic decrease in the specific surface area needed for an effective solid-state reaction.

At mol ratios of 1:6.4 and 1:8 the solid-state reactions forming Sr-hexaferrites are straightforward, as is usually observed during the preparation of Sr-hexaferrites via a solid-state reaction. The large excess of SrO leads to a direct formation of the hexaferrite phase and can be easily extracted with dilute hydrochloric acid after the termination of the solid-state reaction.

However, at low mol ratios the course of the phase formation is widely different and is grounded on the well-known self-sintering phenomenon [12]. The soft magnetic particles of magnetite powder formed in that case represent the major part of the reaction product, exhibiting a hysteresis loop with a very low coercivity, Fig. 7. In addition, in these samples, with a low Sr^{2+}/Fe^{3+} mol ratio, the formation of $SrFe_{12}O_{19}$ at 750 °C, Fig. 1, is strongly hindered. The XRD diffraction spectra and the magnetic measurements show that magnetite is the major phase.

The observed phenomenon, i.e., with a large excess of Sr^2 the Sr-hexaferrite forms, while with a lower excess of Sr^{2+} mostly the iron oxides can be detected, can be linked to the high reactivity of the chemically synthesized iron oxide particles in the starting mixture. Such an otherwise homogeneous precursor mixture might favor, particularly at a low Sr^{2+}/Fe^{3+} mol ratio, the auto sintering of iron oxide powder [13], i.e., the coarsening of the reactive nanoparticles of iron oxide at a temperature lower than that needed to form Sr-hexaferrite at 750 °C, Fig. 1. This process is much more pronounced when the Sr^{2+}/Fe^{3+} mol ratio is low, where the coordination of the iron oxide particles with the same kind of particles is increased. The coarsening of the iron oxide particles leads to a drastic decrease in the iron oxide reactivity, inducing its passivity and strongly delaying the onset of the target solid-state reaction, the formation of Sr-hexaferrite.

Here we recognize that in spite of the chemical method used in our studies the procedure by itself exhibits some peculiarities which lead to the formation of unexpected phases.

During the preparation of fine-grained Sr-hexaferrite via chemical methods a large excess of SrO is required for the suppression of the auto sintering of iron oxide and represents a general demand during the synthesis of iron-oxide-based compounds. Thus, in order to avoid the need for a large excess of SrO during the syntheses of fine-grained particles of Sr-hexaferrite the ''in-situ'' methods [14] have an advantage over other chemical methods.

4. Conclusion

The precursors of the nano-crystalline strontium hexaferrite ($SrFe_{12}O_{19}$) powder were successfully synthesized using the co-precipitation and microemulsion methods. The DTA curve indicated an exothermic peak at 719.3 °C for the sample prepared by the co-precipitation method and at 735.1 °C for the sample prepared by the microemulsion method, which could be attributed to an exothermic reaction and the crystallization of the $SrFe_{12}O_{19}$ hexaferrite particles.

When using both synthesis methods single-phase $SrFe_{12}O_{19}$ was obtained when the hydroxide precursor prepared at a Sr^{2+}/Fe^{3+} mol ratio of 1:8 was calcined at 900 °C.

The $SrFe_{12}O_{19}$ prepared with Sr^{2+}/Fe^{3+} mol ratios of 1:8 and 6.4 had a high saturation magnetization of around 62–64 Am^2/kg and wide hysteresis loops with a coercivity of 5.0–5.4 kOe and remanent magnetization of 36–39 Am^2/kg. Decreasing the Sr^{2+}/Fe^{3+} mol ratio below 1:8 caused a drastic change in the phase composition and consequently in the shape of the hysteresis loop. Here, the magnetite represents the major phase in the product as a consequence of the self-sintering phenomenon in the reaction mixture where the iron oxide represents a large part of the constitutive phases.

References

[1] N. Chen, G. Mu, X. Pan, K. Gan, M. Gu, Microwave absorption properties of $SrFe_{12}O_{19}/ZnFe_2O_4$ composite powders, Mater. Sci. Eng. B 139 (2007) 256–260.
[2] D.H. Chen, Y.Y. Chen, Synthesis of strontium ferrite nanoparticles by coprecipitation in the presence of polyacrylic acid, Mater. Res. Bull. 37 (2002) 801–810.
[3] A. Sharbati, S. Choopani, A.M. Azar, M. Senna, Structure and electromagnetic behavior of nanocrystalline in the 8–12 GHz frequency range, Solid State Commun. 150 (2010) 2218–2222.
[4] D.H. Chen, Y.Y. Chen, Synthesis of strontium ferrite ultrafine particles using microemulsion processing, J. Colloid Interface Sci. 236 (2001) 41–46.
[5] M.M. Hessien, M.M. Rashad, K. El-Barawy, Controlling the composition and magnetic properties of strontium hexaferrite synthesized by co-precipitation method, J. Magn. Magn. Mater. 320 (2008) 336–343.
[6] V.V. Pankov, M. Pernet, P. Germi, P. Mollard, Fine hexaferrite particles for perpendicular recording prepared by the coprecipitation method in presence of an inert component, J. Magn. Magn. Mater. 120 (1993) 69–72.
[7] H. Sato, T. Umeda, Grain growth of strontium ferrite crystallized from amorphous phases, J. Mater. Trans. JIM 34 (1993) 76–81.
[8] G. Elvin, I.P.P. Parkin, Q.T. Bui, L.F. Barquin, Q.A. Pankhurst, A.V. Komarov, Y.G. Morozov, Self-propagating high-temperature synthesis of $SrFe_{12}O_{19}$ from reactions of strontium superoxide, iron metal and iron oxide powders, J. Mater. Sci. Lett. 16 (1997) 1237–1239.
[9] A. Ataie, I.R. Harris, C.B. Ponton, Magnetic properties of hydrothermally synthesized strontium hexaferrite as a function of synthesis conditions, J. Mater. Sci. 30 (1995) 1429–1433.

[10] J. Ding, W.F. Miao, P.G. McCormick, R. Street, High-coercivity ferrite magnets prepared by mechanical alloying, J. Alloys Compd. 281 (1998) 32–36.
[11] C. Surig, K.A. Hempel, D. Bonnenberg, Hexaferrite particles prepared by sol–gel technique, J. IEEE Trans. Magn. 30 (1994) 4092–4094.
[12] U. Natarajan, K. Handique, A. Mehra, J.R. Bellare, K.C. Khilar, Ultrafine metal particle formation in reverse micellar systems: effects of intermicellar exchange on the formation of particles, Langmuir 12 (1996) 2670–3267.
[13] S. Urek, M. Drofenik, Influence of iron oxide reactivity on microstructure development in MnZn ferrites, J. Mater. Sci. 31 (1996) 4801–4805.
[14] M. Drofenik, I. Ban, G. Ferk, D. Makovec, A. Žnidaršič, Z. Jagličić, D. Lisjak, The concept of a low-temperature synthesis for superparamagnetic $BaFe_{12}O_{19}$ particles, J. Am. Ceram. Soc. 93 (6) (2010) 1602–1607.